RSC Advances

RSC Publishing

PAPER

View Article Online
View Journal | View Issue

Cite this: *RSC Advances*, 2013, **3**, 1916

Highly conductive polymer composites from room-temperature ionic liquid cured epoxy resin: effect of interphase layer on percolation conductance

Xinfeng Zhang,*[a] Hongye Sun,[a] Chen Yang,[a] Kai Zhang,[a] Matthew M. F. Yuen*[a] and Shihe Yang*[b]

Received 23rd November 2012,
Accepted 27th November 2012

DOI: 10.1039/c2ra23027e

www.rsc.org/advances

An ionic liquid type imidazolium catalyst enhanced the conductivity of epoxy-anhydride resin based electrical conductive adhesives (ECAs) by more than two orders of magnitude compared with common imidazole compounds. Percolation growth dynamics study combining with epoxy curing kinetics results indicates that the enhancement of conductivity was attributed to the higher percolation efficiency within ionic liquid catalyzed ECAs. An ''interphase layer'' model was proposed to explain the percolation mechanism in the thermoset based conductive composite. The present work highlights the importance of cross-linking the polymer matrix with filler interconnections, and provides practical guidance on the control over percolation dynamics in conductive composites in order to achieve enhanced percolation conductivity.

1. Introduction

Highly conductive polymer composites have attracted considerable interests due to their wide applications in electronic industries such as die attach materials, liquid crystal displays (LCD), and surface-mounted assembly of packaged components on printed wiring board (PWB's).[1–5] Typically those conductive composites contain a polymer matrix filled with conductive fillers. The composite, with composition beyond a critical volume fraction, transits from insulator to conductor while the conductive filler forms a continuous network. This has been well described by connective percolation theory. One of the main disadvantages of the electrical conductive adhesives (ECAs) is their relative high resistivity (10^{-4} Ω cm), compared to eutectic Sn/Pb solders.[6,7] Many efforts have been dedicated to enhance the conductivity of ECAs, *e.g.*, through filler selections and modifications.[6–8]

Curing and thermal treatment are believed to be crucial in electrical conductive performance of ECAs. However, those effects were poorly understood and are still of great controversy. Prior conduction studies[9] have shown that the metallic contacts between silver flakes are primarily established during the cure. Lu *et al.*[10,11] found that cure shrinkage, which brings the silver flake particles closer was the prerequisite. While Inoue *et al.* reported that thermal history has significant effect on electrical conductivity, and the electrical resistivity tends to decrease with increasing curing temperature, even if the samples exhibit full conversion.[12,13] However, it is worth noting that none of the percolation mechanism studies of thermoset composites was based on the dynamic percolation analysis, which might reveal the dynamical formation process of percolation pathways during curing.

In this work, we focus on the study of percolation dynamics in thermosetting epoxy based composites, which is controlled by different catalysts. This is because catalyst affects not only directly the cross-link reaction process, but also the cross-link structure of the resulting polymer matrix (thus indirectly on the physical aging process). It is found that the conductivity of epoxy-anhydride thermoset based composite was greatly affected by catalysts, *i.e.*, much higher conductivity was achieved by ionic liquid catalysts than other common imidazole compounds. This is attributed to the fast growth of percolating network which is largely dependent on the molecular network formation dynamics. Degree of cure (DOC) at gelation was found to be crucial in determining the percolation mechanism. An ''interphase layer'' model was proposed to explain the percolation mechanism in thermoset based conductive composite.

[a]*Department of Mechanical Engineering, The Hong Kong University of Science and Technology, Clear Water Bay, Kowloon, Hong Kong, P. R. China. E-mail: chxzhang@ust.hk; meymf@ust.hk; Fax: +852 2358 1543; Tel: +852 2358 8814*

[b]*Department of Chemistry, William Mong Institute of Nano Science and Technology, The Hong Kong University of Science and Technology, Clear Water Bay, Kowloon, Hong Kong, P. R. China. E-mail: chsyang@ust.hk; Fax: +852 2358 1594; Tel: +852 2358 7362*

2. Experimental section

2.1 Materials

The epoxy used was diglycidyl ether of Bisphenol-A type (DER329, from Shell Chemicals with an average molecular weight of 377). The hardener was anhydride type (hexahydro-4-methylphthalic anhydride, HHMPA). A typical ionic liquid type imidazolium salt, 1-butyl-3-methylimidazolium iodide (BIMI, from Sigma), and three imidazole compounds, 2-ethyl-4-methyl-1*H*-imidazole (EMI, from Sigma), 1-benzyl-2-methylimidazole (BMI, from Sigma), and 1-cyanoethyl-2-ethyl-4-methylimidazole (EMI-CN, from Shikoku Chemicals Corp.) with 0.5 wt% to the epoxy resin weight were used as catalysts for the epoxy curing. Fig. 1 shows the chemical structures of the catalysts adopted in this work. Silver flakes (2–4 μm, supplied by *Sichuan Changcheng Gold*) were used as the conductive filler.

2.2 Preparation of ECAs

For making the ECA samples, a certain amount of silver filler was mixed with epoxy, hardener and catalyst, by using an industrial non-contact ''planetary'' mixer (Thinky mixer, ARE250) for a certain time. In a typical sample preparation process, the epoxy (2.7 g) was mixed with hardener (2.3 g) and Ag flakes (15 g) with the mixer at 2000 rpm for 8 min. Then catalyst (25 mg) was added into the mixture and mixed at 2000 rpm for another 1 min.

2.3 Characterizations

Electrical conductivity was measured with a two-probe method using a Fluke multimeter. The ECA sample was painted onto a glass slide in strips with dimensions of 75 mm × 1 mm × 0.04 mm and cured under the desired conditions. The electrical resistance (R) was measured by the micro ohm meter (Agilent, 34420A); and the electrical resistivity or the electrical conductivity were calculated.

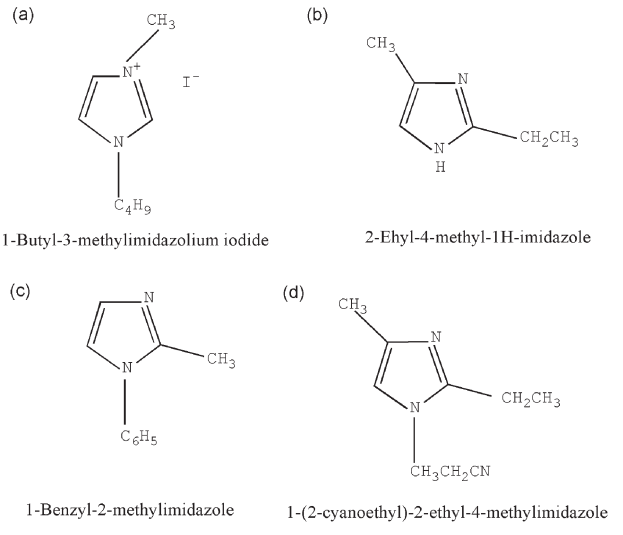

Fig. 1 Molecular structures of (a) 1-butyl-3-methylimidazolium iodide;(b) 2-ethyl-4-methyl-1*H*-imidazole; (c)1-benzyl-2-methylimidazole; (d) 1-(2-cyanoethyl)-2-ethyl-4-methylimidazole.

The percolation dynamics of the ECAs was tested by a Fluke multimeter (Fluke 289). Typically the ECA sample was doctor-bladed into stripes with dimensions of (75 mm × 1 mm) and thickness of 40 μm, onto glass slide with 2 metal electrodes at each end. The ECA sample was then placed on a hotplate and connected to the multimeter by the metal electrodes. The electrical resistivity changes were monitored during the *in situ* curing process under different temperatures.

The curing behaviors of the epoxy were characterized by a differential scanning calorimeter (DSC, TA Q1000). In a typical experiment, around 10–15 mg fresh prepared ECA samples were loaded into the aluminium sample holders and tested from ambient temperature to 250 °C with a ramp rate of 5 °C min^{-1}, to obtain the curing heat flow diagram.

The scanning electron microscopy (SEM) imaging was conducted to observe the morphology of the fracture surface of the cured samples using a JEOL-6300F scanning electron microscope using a 2 kV accelerating voltage. For preparation of the epoxy fracture surface, the epoxy disk samples were cured in a Telfon mold at first. Then the cured epoxy samples were frozen in liquid nitrogen and broken into two halves through the pre-crack at the periphery of the disk. The fractured surfaces were then imaged with SEM.

Gel times of epoxy/Ag ECAs were measured by using a standard test method described in ASTM D3532-99 (2004). Wooden sticks were used to stir the reacting resins by hand every 30 s during the test. The end point was recorded when the reacting resin did not adhere to the end of a clean stick.

Dynamical mechanical analysis (DMA) was tested by a dynamic/thermal mechanical analyzer (Perkin Elmer). The ECAs were cured in a Teflon mold (16.15 mm × 10.95 mm × 0.12 mm dimension) at 150 °C for 1 h for the DMA test. Using the DMA instrument analysis software, the storage modulus, loss modulus, and tan delta curves were obtained.

3. Results and discussions

3.1 Electrical resistivity of composite cured with different types of catalysts

Epoxy-anhydride resin was chosen as the polymer matrix because it is one of the most important types of thermosets due to its superior properties, and wide applications in formulating conductive composites. To study the polymer matrix effect, an ionic liquid type imidazolium salt (BIMI) and three common imidazole compounds were used to catalyze the curing of epoxy-anhydride. This is motivated by the fact that the catalyst will greatly affect the curing and formation dynamics of the polymer network but will not significantly change the chemistry of polymer matrix.[14–17] Fig. 2 collects the electrical resistivity (E_R) of ECAs cured under 150 °C for 15 min with different types of catalysts. The E_R of BIMI-ECA is (4.2 ± 0.4) × 10^{-5} Ω cm, which is almost two orders of magnitude lower than that of the ECAs cured with three common imidazole compounds (of around 10^{-3} Ω cm).

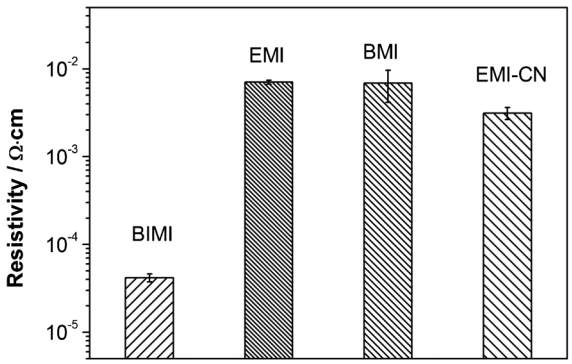

Fig. 2 Resistivity of ECAs cured with different catalysts.

3.2 Curing behaviors of ECAs cured with different catalysts

It is well known that thermal treatment and thermal history of ECAs greatly affect their resistivity. To understand the difference between the ionic liquid BIMI and common imidazoles effect on electrical resistivity of ECAs, the curing behaviors of the epoxy cured with different catalysts were characterized by a DSC dynamic scanning. Here EMI was chosen as a representative for common imidazoles in comparison with ionic liquid BIMI, and the DSC results are given in Fig. 3 and Table 1. We can clearly see that the curing temperature and the heat flow of BIMI-ECA are slightly higher than those of EMI-ECA.

3.3 Percolating network formation dynamics

To study the dependence of the conductive networking formation with epoxy curing, the resistivity of the ECAs cured at different times were collected and plotted with the epoxy curing degree determined from DSC isothermal heating curves, as shown in Fig. 4. BIMI-ECA became conductive within 1 min after curing where the DOC is less than 0.3; and its resistivity dramatically dropped at the beginning 5 min down to 10^{-4} Ω cm. However, EMI-ECA was non-conductive at the first 10 min and became conductive at around 15 min where the DOC had almost reached 1.

Table 1 Curing onset temperature (T_s), curing maximum temperature (T_m), and heat flow (W) of the ECAs cured with BIMI and EMI determined from DSC

Catalyst	T_s (°C)	T_m (°C)	W (Jg^{-1})
BIMI	126.2	153.5	69.6
EMI	130.9	149.7	66.6

From those results, it is obvious that BIMI-ECA has much higher electrical conductivity than EMI-ECA, although its curing speed is even lower than the latter. This suggests that resistivity of ECA was not simply controlled by curing speed and that the resistivity difference in our samples with different catalysts was not due to the curing rate. Our finding disputes the understanding that curing rate was the dominating factors in governing the percolation conductance of composites. The seemingly abnormal phenomenon of the "catalyst dependent" rather than curing rate dependent percolation conductivity promotes us to make a more detailed analysis of the curing effect.

Traditionally the curing of epoxy resin was described more comprehensively by the curing dynamics based on the well-known "Transformation-Time-Temperature" (TTT) diagram,[18] rather than simply the curing rate or curing time. In this scenario, the phase changes of epoxy thermoset, for example, the sol–gel-vitrification transformations are crucial for determining the resin properties. In order to clarify the effect of curing on percolation conductivity, it is of vital importance to relate the conductive percolation to the curing process dynamically, which is shown in Fig. 4.

Fig. 4 illustrates the different conductive networking formation kinetics from BIMI-ECA to EMI-ECA. The composite ECAs transit from an insulator to a conductor while the conductive filler forms a continuous conductive network during the epoxy curing. The networking formation of epoxy resin starts from the gelation due to the growth of infinite cross-linking of the epoxy. The gelation time of BIMI and EMI-ECA under 150 °C were determined and is presented in Fig. 4. It is clearly seen that the DOC at gelation for BIMI-ECA is

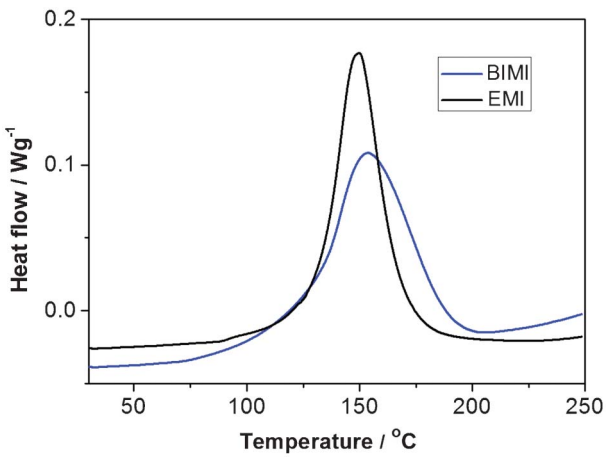

Fig. 3 DSC curves of the ECAs cured with BIMI and EMI.

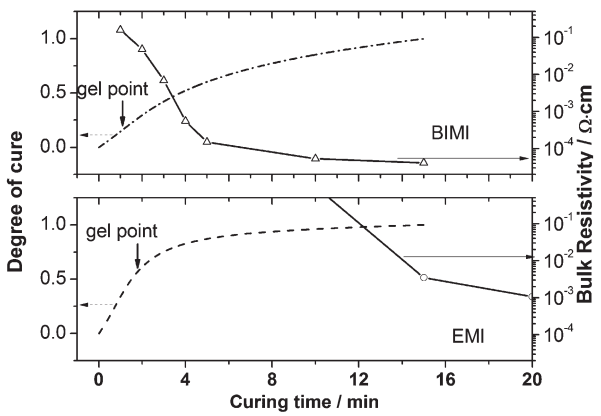

Fig. 4 Isothermal heating curve and degree of cure of the BIMI and EMI-ECA.

around 0.25, which is much smaller than that of EMI-ECA (>0.6). This is similar to the result reported by Zhang *et al.*[17] that an ultralow DOC at gelation was achieved from epoxy-anhydride cured with imidazolium catalyst.

3.4 Effect of DOC on the microstructure of the resulting matrix

The DOC at gelation is one of the most important indices in a thermoset matrix. At the molecular level, different DOC at gelation reflects the difference in gel structure. Generally a high DOC at gelation is due to the formation of microgels at the pre-gel stage. A high DOC at gelation generates microgel domains which lead to inhomogeneity in the final polymer networking composed of cross-linked rich domains surrounded by less cross-linking interface.[19] While a low DOC at gelation favors the formation of more uniform networking. Fig. 5a and b plot the corresponding structure formed at low and higher DOC at gelation. To reveal the cross-linked structure difference, the fracture surface of pure epoxy cured with BIMI and EMI were imaged by SEM which are given in Fig. 5c and d. It is clearly shown that BIMI cured epoxy has a more uniform and smooth structure, while the surface of EMI cured epoxy is rough and composed of many domains.

The difference in the polymer cross-link structures was further proved by a DMA study. Fig. 6 shows the DMA curves for BIMI-ECAs and EMI-ECAs. The storage modulus (E') for BIMI-ECAs is much larger than that of EMI-ECAs. Since E' can be related in a homogeneous polymer with the molar mass of the network chains by the theory of rubber elasticity (eqn 1):

$$E' = 3RT\rho/M_c \quad (1)$$

where R is the gas universal constant, ρ is the density, and M_c is the molar mass of the network chains (*i.e.*, the molar mass between crosslinks). Although this theory cannot be applied to a nonhomogeneous system, we have used M_c as an indication of the apparent crosslinking density.[20,21] The calculated cross link density of BIMI-ECA is about 2 times larger than that of EMI-ECA, indicating that BIMI-ECA is more rigid than EMI-ECA. Furthermore, the height of the peak of tan δ(damping) for BIMI-ECA is lower than that of EMI-ECA. EMI-ECA possesses higher damping than BIMI-ECA, and it is reflected in the greater flexibility of EMI-ECA with the formation of micro domain network.

Note that recently Anuar *el al.*[22] reported the effect of the types of epoxy on electrical conductivity of silver filled ECAs and found that the ECA cured with amine adducts has a much higher conductivity than that cured with another kind of liquid amine curing agent (Jeffamine). In their case, they directly correlated the electrical conductivity to the cross-link density of the epoxy matrix. However, we note that great care should be taken while simply relating the percolation conductivity to the mechanical properties of the matrix. The first reason is that, the cross-link density determined from storage modulus according to the theory of rubber elasticity is based on the assumption of a uniform cross-link polymer structure, which might not be fulfilled by the real samples. The second reason is that the simple calculation of cross-link density according to equation 1 neglects the contribution of filler network to the composites. So we didn't intend to correlate the conductivity of ECAs to their storage modulus.

3.5 Percolation model for silver-epoxy

Those results shown above indicate that the DOC at gelation is like the physical origins in inducing the difference in percolation dynamics. We proposed an ''interphase layer'' model to explain the percolation behaviors under different DOC at gelation, as illustrated in Fig. 7. Before curing, the interphase layer has not been formed between fillers. On curing, an interphase layer can be solidified and becomes a barrier layer between the fillers. With lower DOC at gelation, the filler was connected upon the compressive stress and could form good metallic contact due to the large fraction of polymer sol (Fig. 7a and b). However, for higher DOC at gelation, due to the relatively low sol fraction, a cross-linked interphase layer might be formed and intercalated between the filler contacts (Fig. 7c and d). In the latter case, the

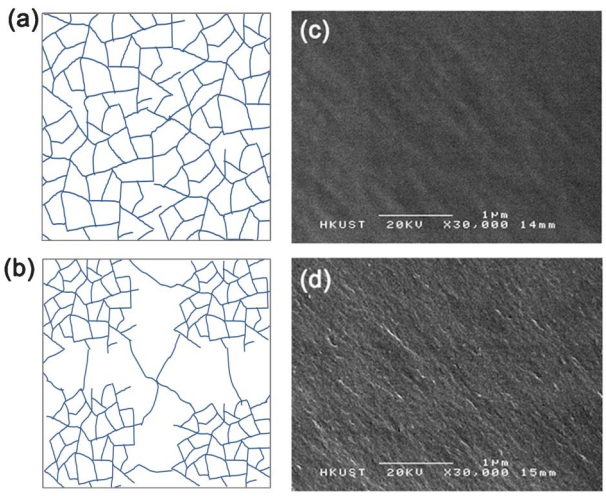

Fig. 5 Schemes of the cross-linked structure of the matrix with (a) low DOC at gelation; and (b) high DOC at gelation. (c) and (d) are the SEM images of the fractured surface of the epoxy cured with BIMI and EMI.

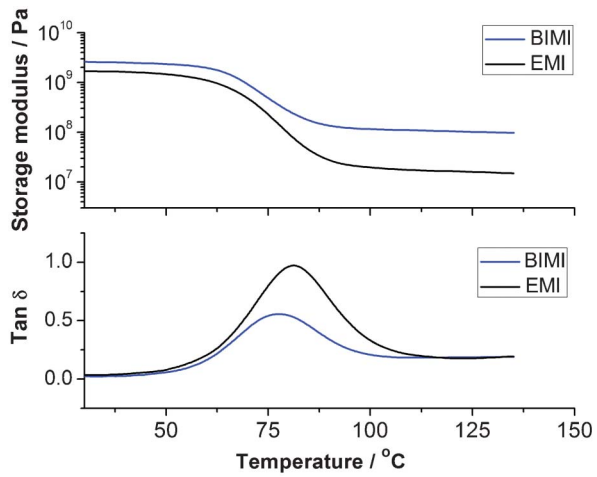

Fig. 6 DMA results of the ECAs cured with BIMI and EMI.

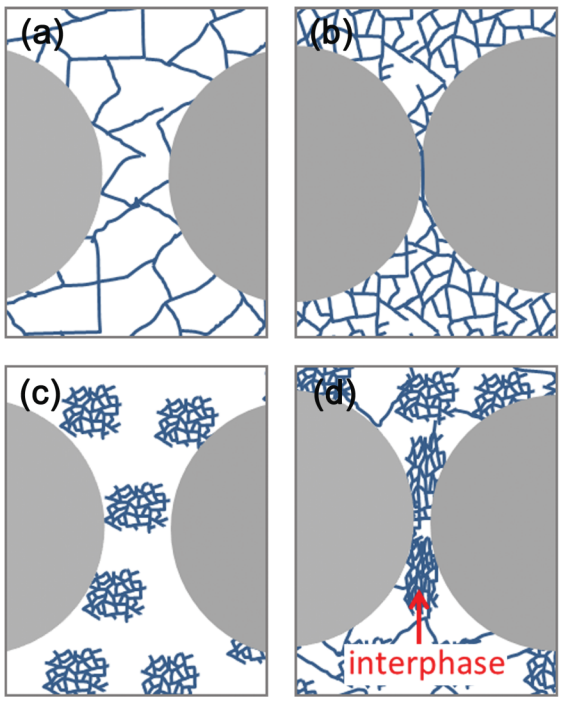

Fig. 7 (a) and (b) illustrate the filler percolation before gelation and after curing with low DOC at gelation in BIMI-ECA. With the small percentage of gel fraction (<30%) and large amount of sol fraction (>60%) at gelation point (a), the fillers form good metallic contact between each other (b), resulting in ultrahigh electrical conductivity. (c) and (d) illustrate the filler percolation before gelation and after curing with high DOC at gelation in EMI-ECA. Due to the large amount of gel fraction (>60%), fillers could not penetrate the gel layer. An interphase layer forms between the fillers after curing, which greatly increases the resistivity of ECA.

presence of the interphase layer greatly deteriorates the electrical conductance due to the loss of direct metallic contact between the fillers.[23]

Noting that the model described in Fig. 7 is a rough picture on the effect of kinetically produced interphase layer on intercontact between fillers. In the real composite system, it is most likely that the filler–filler contact will be deviated from the direct metal contact, due to the chemical bonded surfactants or chemical/physical adsorbed polymer molecules during the mixing process. However, those thermodynamically induced surface layers on the fillers will not be kinetically controlled by the curing process, thus will not contribute to the kinetically produced interphase layer.

It is the first time that kinetically produced interphase layer was proposed to understand the percolation conductivity of thermoset based conductive composites, basing on the percolation kinetic study. This model is quite similar to a previously reported percolation model in carbon-black filled thermoplastics composites.[24] In that work by Wu *et al.*,[24] the authors have studied the dynamic process of forming conductive networks in carbon-black filled thermoplastic composites. They observed that the percolation dynamics of carbon-black is directly related to the zero-shear-rate viscosity of the polymer matrix, which affected the "interphase layer" between the carbon-black fillers and finally the percolation dynamics. The major difference between their model and ours is that the mobility of the polymer chain determines the interphase layer thickness in thermoplastic composite; while the curing induced microstructure of the matrix determines interphase layer thickness in thermoset (like epoxy resin) based composites. The proposed interphase model for thermoset based conductive composites is likely to provide practical guidance on the control over percolation dynamics in conductive composites in order to achieve enhanced percolation conductivity.

3.6 Thermal effect on electrical percolation

The electrical resistivity of EMI and BIMI-ECAs shows different dependence on thermal effects, as shown in Fig. 8: the resistivity of BIMI-ECAs is almost independent of the curing temperature, while the EMI-ECAs decreased sharply from 10^{-2} to 10^{-4} Ω cm with an increase of temperature from 150 to 190 °C. This can be understood by the fact that the domain-composed inhomogeneity of the polymer matrix is sensitive to thermal treatment and higher temperature physical aging is beneficial for the repositioning of the interphase layer and reducing the barriers between the fillers.[19]

3.7 Practical guidance from Time-Temperature-Transformation (TTT) diagram

The proposed interphase layer model could explain the reaction-controlled and physical aging-controlled percolation mechanisms. It suggests that the percolation dynamics could be controlled through the DOC at gelation. It is well known that the TTT diagram has become a standard concept to describe the curing behaviors of thermosets.[18] It suggests that the TTT diagram can be used to provide practical guidance on the control over the percolation dynamics of thermoset based conductive composites.

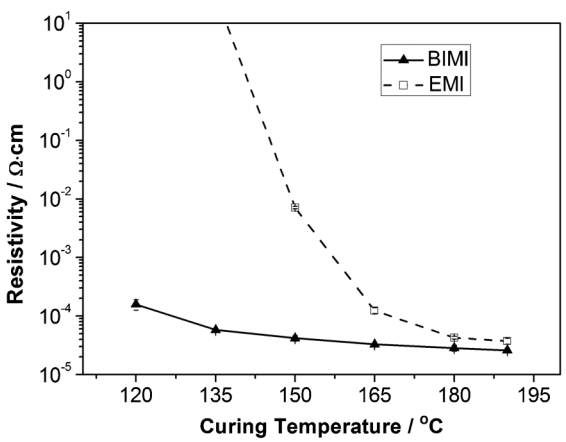

Fig. 8 Evolution of the electrical resistivity of ECAs cured with BIMI and EMI under increased curing temperature.

4. Conclusions

In summary, the epoxy-anhydride type resin based ECA catalyzed by ionic liquid type imidazolium salt decreased in its electrical resistivity by almost two magnitudes in comparison with ECAs catalyzed by other common imidazole compounds. The ionic liquid catalyzed epoxy resin gelled at a low degree of cure, favoring the formation of a conductive network. An interphase layer model was proposed according to these findings to illustrate the discrepancies in percolation dynamics.

References

1 Y. Li, K. Moon and C. P. Wong, *Science*, 2005, **308**, 1419.
2 J. M. Kim, K. Yasuda and K. Fujimoto, *J. Electron. Mater.*, 2005, **34**, 600.
3 L. Q. Cao, Z. H. Lai and J. H. Liu, *J. Electron. Packag.*, 2005, **127**, 43.
4 Y. Li, K. S. Moon and C. P. Wong, *J. Electron. Mater.*, 2005, **34**, 266.
5 H. Chiang, C. Chung, L. Chen, Y. Li and C. P. Wong, *J. Adhes. Sci. Technol.*, 2005, **19**, 565.
6 H. Jiang, K. S. Moon, Y. Li and C. P. Wong, *Chem. Mater.*, 2006, **18**, 2969.
7 R. Zhang, K. S. Moon, W. Lin and C. P. Wong, *J. Mater. Chem.*, 2010, **20**, 2018.
8 R. Zhang, W. Lin, K. S. Moon and C. P. Wong, *ACS Appl. Mater. Interfaces*, 2010, **2**, 2637.
9 D. Klosterman and L. Li, *J. Electron. Manuf.*, 1996, **5**, 277.
10 D. Lu and C. P. Wong, *International Symposium on Advanced Packaging Materials*, 1999, 295.
11 D. Lu, Q. K. Tong and C. P. Wong, *International Symposium on Advanced Packaging Materials*, 1999, 2.
12 M. Inoue and K. Suganuma, *J. Electron. Mater.*, 2007, **36**, 669.
13 M. Inoue, H. Muta, T. Maekawa, S. Yamanaka and K. Suganuma, *J. Electron. Mater.*, 2008, **37**, 462.
14 M. A. M. Rahmathullah, A. Jeyarajasingam, B. Merritt, M. Van Landingham, S. H. McKnight and G. R. Palmese, *Macromolecules*, 2009, **42**, 3219.
15 K. Kowalczyk and T. Spychaj, *Polimery*, 2003, **48**, 833.
16 F. Ricciardi, W. A. Romanchick and M. M. Joullie, *J. Polym. Sci., Polym. Lett. Ed.*, 1983, **21**, 633.
17 Z. Zhang, E. Beatty and C. P. Wong, *Macromol. Mater. Eng.*, 2003, **288**, 365.
18 M. T. Aronhime and J. K. Gillham, *Adv. Polym. Sci.*, 1986, **78**, 83.
19 C. M. Sahagun and S. E. Morgan, *ACS Appl. Mater. Interfaces*, 2012, **4**, 564.
20 L. Rey, J. Duchet, J. Galy, H. Sautereau, D. Vouagner and L. Carrion, *Polymer*, 2002, **43**, 4375.
21 M. L. Auad, M. Aranguren and J. Borrajo, *J. Appl. Polym. Sci.*, 1997, **66**, 1059.
22 S. K. Anuar, M. Mariatti, A. Azizan, N. C. Mang and W. T. Tham, *J. Mater. Sci.: Mater. Electron.*, 2011, **22**, 757.
23 D. Toker, D. Azulay, N. Shimoni, I. Balberg and O. Millo, *Phys. Rev. B*, 2003, **68**, 041403.
24 G. Wu, S. Asai, C. Zhang, T. Miura and M. Sumita, *J. Appl. Phys.*, 2000, **88**, 1480.